

electro-optical GaAs–AlGaAs waveguide optical phased array fabricated on a single chip by Chiaro Networks.¹² It contains a set of 18 subarrays, each comprising 128 waveguides that can be individually electrically biased by means of a set of digital-to-analog converters. The device is used by Chiaro for optical switching and was modified to serve as an array of $18 \times 128 = 2304$ phase modulators by removal of the fibers and part of the fiber-to-waveguide coupling optics. The 12.5 mm long ridge waveguides were created by photolithography and subsequent reactive-ion etching. Each waveguide is $9 \mu\text{m}$ wide, and the separation between waveguides is $2 \mu\text{m}$, eliminating waveguide-to-waveguide coupling. The gaps (dead zones) between adjacent subarrays are $194 \mu\text{m}$ wide. These gaps are the result of the specific Chiaro application requirements and are not due to any technological limitations. The structures were formed upon a multilayer AlGaAs structure grown on an N^+ -doped GaAs wafer. Details of the fabrication method can be found elsewhere.¹³

The optical components that were not removed from Chiaro's device are aspheric cylindrical lenses (L4 and L5; Fig. 1) used for coupling light into and out of the waveguides along the vertical axis. For best coupling into the waveguide array, we had to produce a flat phase front spot with vertical dimensions of $450 \mu\text{m}$ on lens L4. For that purpose we used a telescopic relay with cylindrical lenses L1 and L2 that imaged the output coupler of the laser onto lens L4. Aspheric cylindrical lens L4 then focused the beam down to about $2 \mu\text{m}$, coupling the light efficiently into the waveguide. To decrease the Fresnel reflection losses from the waveguides, we coated the device edges with single-layer antireflection coating. The overall loss of the phased array of ~ 7 dB is due mainly to free-space-to-waveguide coupling loss, Fresnel reflection loss from the waveguide's facets, and the dead zones. We believe that we could significantly reduce the loss by optimizing the lens design and customizing the waveguide array for this specific application. Note that in this design the cylindrical optics separate the functions of the Fourier lenses (obtained by 250 mm cylindrical lenses L3 and L6) and the coupling into the $2 \mu\text{m}$ waveguides over the entire spectral bandwidth in the Fourier plane; 830 mm^{-1} gold-coated gratings blazed for 1260 nm (G1, G2) were used to spectrally disperse the light.

The horizontal spot size of a single-wavelength component was $\sim 50 \mu\text{m}$. It covered approximately five individual waveguides. This 5:1 ratio of spot size to waveguide width enables both phase and amplitude to be manipulated on the individual spectral components.¹ High diffraction orders resulting from the discreteness of the waveguides are blocked by the finite aperture of Fourier lens L6. We used a mode-locked Cr:F laser centered about 1250 nm with an ~ 27 nm bandwidth. This spectrum spanned ~ 10 nm horizontally in the Fourier plane, illuminating ~ 6 subarrays (a total of ~ 700 waveguides), permitting $700/5 = 140$ degrees of freedom for complete (phase and amplitude) modulation. Note that this device can

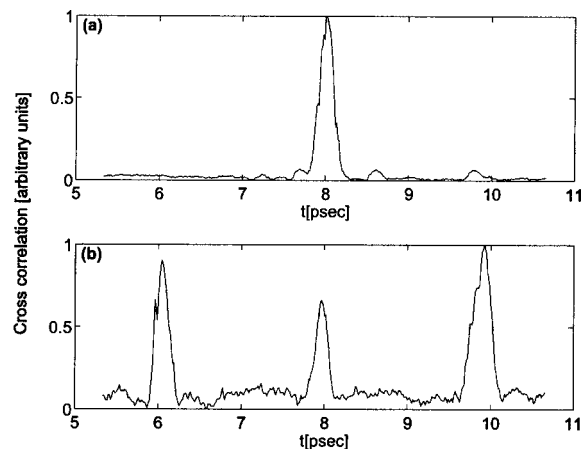


Fig. 2. Experimental cross-correlation results. (a) Only lookup table voltages encoded into the phase array. (b) Cosine phase-modulated mask encoded into the phase array.

provide as many as $2304/5 \approx 460$ degrees of freedom if the laser spectrum is spanned over the entire array.

The light emerging from the unbiased waveguides shows phase variations that result from stress induced by electrical contacts on the individual guides. Therefore, by maximizing a second-harmonic signal, we calibrated the device to flatten the output phases. The resultant lookup table was used as the zero-phase starting point in further experiments.

To test the shaping capability of the device, we encoded various phase functions into the array. The shaped pulses were cross correlated with unshaped pulses from the laser in a noncollinear second-harmonic setup. Typical results are shown in Fig. 2. Figure 2(a) shows cross-correlation traces with just zero-phase voltages encoded into the phase array. Figure 2(b) shows a typical result for a cosine phase mask, i.e., $\varphi(\omega) = A \cos[B(\omega - \omega_0)]$. Such harmonic phase modulation produces a series of pulses with relative amplitude proportional to $J_n(A)$ for the n th pulse. This relative amplitude distribution is further apodized as the result of the finite spot size in the Fourier plane.¹ In Fig. 2(b) the three cross-correlation peaks are due to the zero and first orders. The distance between the pulses is ~ 1.9 ps, as expected. Other sinusoidal phase masks with different periods and (or) modulation depths (A) yielded results that were predicted by theory. To experimentally verify the modulation capability of the shaper we encoded a binary phase grating with a period (two waveguides) that is smaller than the single-wavelength spot size (approximately five waveguides). By varying the relative phase $\delta\varphi$ between adjacent waveguides, one can precisely control the ratio between the amount of light that is diffracted to the zeroth order and higher orders. We therefore have precise control of the amplitude, as only the zeroth order is within the temporal window defined by the single-wavelength spot size. Using this technique, one could theoretically obtain complete attenuation of a specific frequency component for $\delta\varphi = \pi$. We experimentally achieved an intensity attenuation of 15 dB.

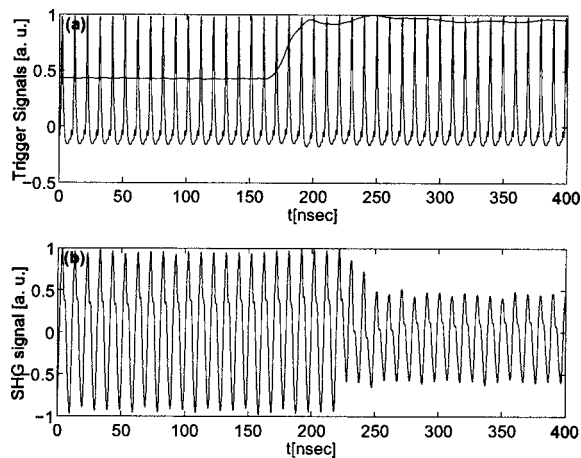


Fig. 3. Rise-time measurements. (a) Trigger signals: laser pulses and voltage on the waveguide. (b) Second-harmonic transient measurement.

In a second experiment we tested the update speed. The electronics that we used limited us to changing the phases of only one subarray for each computer command. Therefore we narrowed the spectrum to just three subarrays (a total of 384 waveguides), using a slit in the Fourier plane and thus utilizing ~ 15 nm of the pulse spectrum. We then encoded a π step into the central waveguide array. The output of the shaper was focused by a 50 mm lens into a 1 mm thick lithium iodate crystal. The second harmonic from the crystal was filtered and directed into a fast photomultiplier tube. However, the nonlinear signal produced in a single-shot experiment turned out to be quite weak and noisy. We therefore averaged our measurements over 1000 events.

Figure 3 shows the drop in the second-harmonic generation (SHG) signal as the phase-step command is applied. The top figure shows the 100 MHz mode-locked pulse train and the voltage step applied to the device. The lower figure shows the SHG response. The pulse shape was configured in ~ 30 ns, a time that was limited only by the driving electronics. The ratio of second-harmonic signal amplitudes for unshaped and shaped pulses is 1.6, in excellent agreement with the expected decrease in the SHG signal for this pulse shape. Along with the second-harmonic measurements we also measured the linear intensity for shaped and unshaped pulses. We found the shaped pulse intensity to be $\sim 3\%$ less than that of an unshaped pulse. We attribute this loss to the diffraction in the Fourier plane that is due to the π phase steps in the case of the shaped pulse.

In summary, we have shown that a GaAs phased-array modulator can be used as a phase-and-

amplitude pulse shaper with a large number of controlled degrees of freedom, comparable to today's high-end liquid-crystal modulators. The modulation speed is many orders of magnitude higher than any other technique used today and is close to the desired sub-10 ns scale on which every single pulse from the femtosecond oscillator could be independently shaped. The experimentally demonstrated ~ 30 ns update time scale is far from being a physical limit in this device and is simply due to limitations of the driving electronics that are currently available. We estimate that modulation speeds of the order of 1 ns, similar to that of typical electro-optical modulators, are attainable. On the downside, we note the necessity to couple the light in a vertical direction into the waveguides, requiring special precision mechanical assembly. We expect that such fast-rate shaping modulation will open new avenues in fields of research such as selective chemistry, coherent control, nonlinear scanning microscopy, and optical communications.

We gratefully acknowledge financial support by the Israel Science Foundation. E. Frumker's e-mail address is evgenyf@weizmann.ac.il.

References

1. A. M. Weiner, *Rev. Sci. Instrum.* **71**, 1929 (2000).
2. A. M. Weiner, J. P. Heritage, and J. A. Salehi, *Opt. Lett.* **13**, 300 (1988).
3. A. Assion, T. Baumert, M. Bergt, T. Brixner, B. Kiefer, V. Seyfried, M. Strehle, and G. Gerber, *Science* **282**, 919 (1998).
4. D. Meshulach and Y. Silberberg, *Nature* **396**, 239 (1998).
5. P. Tian, D. Keusters, Y. Suzuki, and W. S. Warren, *Science* **300**, 1553 (2003).
6. N. Dudovich, D. Oron, and Y. Silberberg, *Nature* **418**, 512 (2002).
7. A. M. Weiner, D. E. Leaird, J. S. Patel, and J. R. Wullert II, *Opt. Lett.* **15**, 326 (1990).
8. E. Zeek, K. Maginnis, S. Backus, U. Russek, M. Murnane, G. Mourou, H. Kapteyn, and G. Vdovin, *Opt. Lett.* **24**, 493 (1999).
9. C. W. Hillegas, J. X. Tull, D. Goswami, D. Strickland, and W. S. Warren, *Opt. Lett.* **19**, 737 (1994).
10. E. Frumker, D. Oron, D. Mandelik, and Y. Silberberg, *Opt. Lett.* **29**, 890 (2004).
11. T. Brixner and G. Gerber, *Opt. Lett.* **26**, 557 (2001).
12. G. Matmon, G. Tidhar, D. Majer, E. Shekel, and S. Ruschin, presented at the 28th European Conference on Optical Communications, Sept. 8–12, 2002, Copenhagen, Denmark.
13. A. Feingold, D. Majer, A. Arbel, A. Grinman, M. Altman, J. Levy, and E. Shekel, in *The 2004 International Conference on Compound Semiconductor Manufacturing* (GaAs MANTECH, 2004), p. 239.